**NASA TECHNICAL MEMORANDUM**

**NASA TM X-62,431**

NASA TM X-62,431

# EXPERIMENTAL STUDY OF THE EFFECT OF SPAN LOADING ON AIRCRAFT WAKES

Victor R. Corsiglia, Vernon J. Rossow, and Donald L. Ciffone

Ames Research Center
Moffett Field, California 94035

May 1975

| 1. Report No. | 2. Government Accession No. | 3. Recipient's Catalog No. |
|---|---|---|
| NASA TM X-62,431 | | |

| 4. Title and Subtitle | 5. Report Date |
|---|---|
| EXPERIMENTAL STUDY OF THE EFFECT OF SPAN LOADING ON AIRCRAFT WAKES | 6. Performing Organization Code |

| 7. Author(s) | 8. Performing Organization Report No. |
|---|---|
| Victor R. Corsiglia, Vernon J. Rossow, and Donald L. Ciffone | A-6064 |
| | 10. Work Unit No. 514-52-01 |

| 9. Performing Organization Name and Address | 11. Contract or Grant No. |
|---|---|
| Ames Research Center, NASA<br>Moffett Field, California 94035 | |
| | 13. Type of Report and Period Covered<br>Technical Memorandum |

| 12. Sponsoring Agency Name and Address | 14. Sponsoring Agency Code |
|---|---|
| National Aeronautics and Space Administration<br>Washington, D.C. 20546 | |

15. Supplementary Notes

Presented at AIAA 8th Fluid and Plasma Dynamics Conference, Hartford, Conn., June 16–18, 1975

16. Abstract

Measurements were made in the NASA-Ames 40- by 80-Foot Wind Tunnel of the rolling moment induced on a following model in the wake 13.6 spans behind a subsonic transport model for a variety of trailing edge flap settings of the generator. It was found that the rolling moment on the following model was reduced substantially, compared to the conventional landing configuration, by reshaping the span loading on the generating model to approximate a span loading, found in earlier studies, which resulted in reduced wake velocities. This was accomplished by retracting the outboard trailing edge flaps. It was concluded, based on flow visualization conducted in the wind tunnel as well as in a water tow facility, that this flap arrangement redistributes the vorticity shed by the wing along the span to form three vortex pairs that interact to disperse the wake.

| 17. Key Words (Suggested by Author(s)) | 18. Distribution Statement |
|---|---|
| Aircraft wake turbulence<br>Wake turbulence<br>Aircraft trailing vortices<br>Vortex | Unclassified – Unlimited<br>STAR Category – 02, 01 |

| 19. Security Classif. (of this report) | 20. Security Classif. (of this page) | 21. No. of Pages | 22. Price* |
|---|---|---|---|
| Unclassified | Unclassified | 11 | $3.25 |

*For sale by the National Technical Information Service, Springfield, Virginia 22151

# EXPERIMENTAL STUDY OF THE EFFECT OF SPAN LOADING ON AIRCRAFT WAKES

Victor R. Corsiglia,* Vernon J. Rossow,† and Donald L. Ciffone‡
Ames Research Center, NASA, Moffett Field, California 94035

## Abstract

Measurements were made in the NASA-Ames 40- by 80-Foot Wind Tunnel of the rolling moment induced on a following model in the wake 13.6 spans behind a subsonic transport model for a variety of trailing edge flap settings of the generator. It was found that the rolling moment on the following model was reduced substantially, compared to the conventional landing configuration, by reshaping the span loading on the generating model to approximate a span loading, found in earlier studies, which resulted in reduced wake velocities. This was accomplished by retracting the outboard trailing edge flaps. It was concluded, based on flow visualization conducted in the wind tunnel as well as in a water tow facility, that this flap arrangement redistributes the vorticity shed by the wing along the span to form three vortex pairs that interact to disperse the wake.

## Nomenclature

$AR$ = aspect ratio, $b^2/S$

$b$ = span of wing

$c$ = wing chord

$\bar{c}$ = average chord, $S/b$

$C_l$ = rolling-moment coefficient, torque/$\left(\frac{1}{2}\rho U_\infty^2 Sb\right)$

$C_L$ = lift-coefficient, lift/$\left(\frac{1}{2}\rho U_\infty^2 S\right)$

$S$ = wing area

$t$ = time

$U_\infty$ = free-stream velocity (aligned with x axis)

$x,y$ = coordinate axes; x is streamwise and y is spanwise

$\alpha$ = angle of attack

$\Gamma$ = circulation

$\rho$ = air density

Subscripts

$f$ = following model that encounters wake

$g$ = model that generates wake

## Introduction

The trend toward higher air traffic density at airports coupled with the widening range in aircraft size increases the hazard to small aircraft that might encounter a large aircraft's trailing wake vortices. One form of the hazard is an overpowering rolling moment on the encountering aircraft. The Department of Transportation is studying means for locating these vortices in order to vector aircraft away from the vortex wake and to establish safe operating distances. The NASA effort has concentrated on the study of possible ways to reduce the rolling moment on an encountering aircraft to a controllable level. Initial investigations have been directed at finding possible ways to accomplish this by changing the generating aircraft configuration only slightly in what would be considered a retrofit modification. As a part of this study, the investigation reported herein considers a variety of flap configurations on a typical subsonic jet transport in an attempt to determine whether the vortex wake is significantly modified by the span loading changes that are possible with the existing flap system. Other methods for alleviating the vortex wake intensity, such as turbulence injection into the vortex[1,2,3] and initiation of vortex instabilities by oscillating the wing geometry,[4,5] are not reported here.

The application of span load modification to the present configuration was stimulated and guided by recent theoretical studies[6,7] that predict a significant reduction of the velocities in the wake by a redistribution of the spanwise loading on the generating wing. These results were confirmed in a later experimental study of the wake of a swept wing in a water tow facility.[8] In the present experiments, the span loadings produced by independently changing the deflection of the trailing edge flaps can be considered as approximations to the span loadings that were found, theoretically, to yield large vortex cores and interactions between multiple vortices. The subsonic transport model used in the present tests to generate the vortices is representative of a B747 airplane. As the lift on this generating model was varied by changing the angle of attack, the rolling moment on several following aircraft models was measured at several vertical and lateral locations in the wake. The technique used here is similar to that of Wentz,[9] Singh,[10] Banta,[11] Iversen,[12] and Dunham.[13] The work of Dunham (carried out concurrently) uses identical generator and follower models. Dunham's rolling-moment experiments differ, however, in that his models are towed through water, and his results extend to greater downstream distances.

## Apparatus and Test Procedure

### Wind-Tunnel Setup

A schematic diagram of the experimental setup is shown in Fig. 1 with the generator model at the forward end of the test section and following model at the exit of the test section of the NASA-Ames Research Center 40- by 80-Foot Wind Tunnel. The generator model is centrally located in the inlet and is attached by a single strut through a straingage balance to measure lift. The angle of attack of the generator was set remotely through an actuator and indicator. Downstream of the generator model 24.4 m (80 ft), a follower model was mounted on a single strut that could be remotely positioned vertically over a 3.05 m (10 ft) range and laterally over a 4.27 m (14 ft) range. Additional geometric details of the follower models are given in Table 1. The follower model was attached to its strut through a strain-gage balance to measure rolling moment. Full-scale range for the balance was such that adequate sensitivity would be provided for the rolling moment encountered on each model (see Table 1). The following model was constructed of balsa wood to ensure a high-frequency response, and, as a result, the natural frequency of the model balance combination (31 Hz, model 1) was several

*Aerospace Engineer. Member AIAA.
†Staff Scientist. Associate Fellow AIAA.
‡Aerospace Engineer.

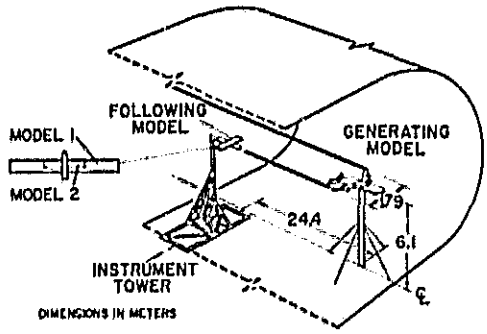


Fig 1 Experimental setup in the NASA Ames 40- by 80-Foot Wind Tunnel.

Table 1 Model Dimensions and Wind-Tunnel Conditions

| | | |
|---|---|---|
| Model dimensions | | |
| Following model | 1 | 2 |
| Span, cm (in.) | 87.4 (34.4) | 33.3 (13.1) |
| Chord, cm (in.) | 9.8 (3.9) | 6.1 (2.4) |
| Aspect ratio | 8.9 | 5.5 |
| Wing section | NACA 0012 | NACA 0012 |
| Fuselage diameter, cm (in.) | 5.1 (2.0) | 5.1 (2.0) |
| Balance full-scale range, N-m (in.-lb) | 11.3 (100) | 3.4 (30) |
| Generator model | | |
| Wing | | |
| Span, cm (in.) | 179 (70.5) | |
| Root incidence | +2° | |
| Tip incidence | −2° | |
| Area, $m^2$ ($ft^2$) | 0.459 (4.94) | |
| Average chord, cm (in.) | 25.6 (10.1) | |
| Aspect ratio | 7 | |
| Horizontal stabilizer | 0° | |
| Wind-tunnel conditions | | |
| $U_\infty$, m/s (ft/sec) | 40 (131) | |
| Reynolds number based on average chord | $7\times10^5$ | |

times larger than rolling moment frequencies encountered. The subsonic transport model (Fig. 2) that was used as the wake vortex generator was equipped with two spanwise segments of triple-slotted trailing edge flaps, capable of providing high lift. Full-span leading edge slats were installed when the trailing edge flaps were deflected.

## Rolling-Moment Measurement

The procedure for recording the rolling moment consisted of setting the generator model and wind-tunnel conditions and selecting a lateral and vertical position for the following model. The time-varying rolling-moment signal was recorded on a light-beam strip-chart recorder. Sufficient length of record was taken to obtain the highest or peak rolling moment for that location (usually about 1 min). The procedure was then repeated at successive lateral and vertical positions of the aft model in about

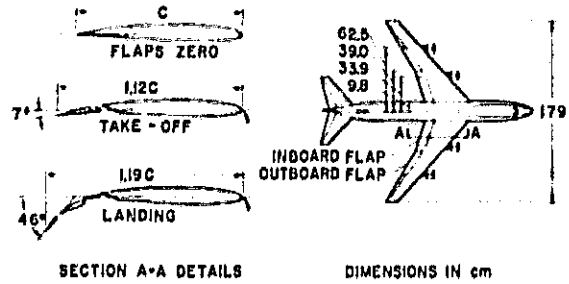


Fig. 2 Geometric details of the subsonic transport model (dimensions in cm).

10 cm (4 in.) increments to determine the maximum value of rolling moment for each condition. Figure 3 shows a typical record of rolling-moment variation with time. The source of the unsteadiness of the rolling moment signals is the meander of the vortices in the wind tunnel due to wind tunnel turbulence. Earlier studies have shown[3] that single vortices can move about as much as 1 m (3.3 ft). The peak rolling moment values shown on Fig. 3 are interpreted as corresponding to the times when the following model is aligned with a vortex center. During the 38 sec of data shown, the peak rolling moment was repeated three times.

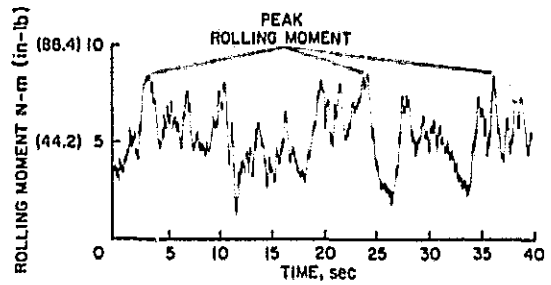


Fig. 3 Typical record of rolling moment induced on following model 1 as a function of time; generator flaps: Ldg/Ldg.

The generator model was tested in both the upright and inverted positions to evaluate strut interference effects. It was found that for the conventional configurations, where the vortices are shed primarily from the wing tip region, that no strut interference could be found. However, for the configurations with the span loading shifted inboard, in which vortices are shed inboard of the wing tip, an inverted mounting of the generator model was required to avoid interference caused by the wake of the model mounting strut. Figure 1 shows the generator model in this inverted position.

## Flow Visualization

Wind Tunnel. The form and motion of the vortices in the wake of several configurations of the subsonic transport model were studied by the use of smoke (i.e., a vaporized oil mist) inserted into the stream by a rake (not shown in Fig. 1) located just ahead of the generator model. Oil was pressure fed to the rake and vaporized electrically before being expelled into the stream through a number of small tubes in the trailing edge of the rake. Since the rake also had a span of about 1.8 m (5.9 ft), the smoke flowed over the entire wing, thereby marking the wake. A light slit that produced a sheet of light normal to the wake was used at several downstream stations to observe the structure of the vortices. The rake and its supports were removed before rolling moment measurements were made.

Water Tow Facility. Flow visualization studies were also conducted by underwater towing of an identical model scaled to a 0.61 m (2 ft) span. This facility (located at the University of California's Richmond Field Station) allows flow visualization to greater downstream distances than are possible in the wind tunnel. The water tank dimensions are 1.8 X 2.4 m (6 X 8 ft) and is 61 m (200 ft) long. Tow velocities of up to 2 m/sec (6.6 ft/sec) were used. Dye was emitted at the wing tips as well as the inboard and outboard edges of the trailing edge flaps, and the light slit apparatus was again used to identify the wake structure.

## Discussion of Results

The span loadings produced by various flap settings of the generator were first computed using a vortex lattice method for the wing and flaps, including the effects of camber and twist, but without fuselage or tail. The predicted effect of various flap combinations on span loading is shown in Fig. 4. It is noted that the conventional flaps 0° and take-off configurations have approximately elliptical span loading and hence would be expected to shed a single vortex from each wing tip.[6] With the conventional landing configuration, some additional sharp gradients in loading are evident at the flap edges, from which discrete vortices might originate. However, with one flap retracted [Fig. 4(b)], these gradients are more pronounced and three vortices from each wing would be expected, i.e., one from each flap edge and one from the wing tip.

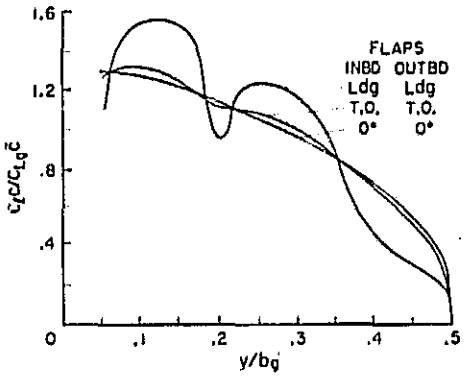


(a) Conventional configurations.

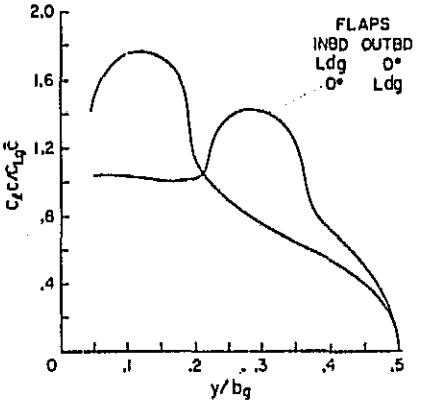


(b) Modified configuration.

Fig. 4 Predicted span loadings on the subsonic transport model for several flap settings.

Next, the variation of the lift coefficient with angle of attack was measured (Fig. 5). The reduction in lift curve slope for all configurations above $\alpha = 8°$ corresponds to the onset of flow separation on the wing-tip region which was observed with the aid of tufts.

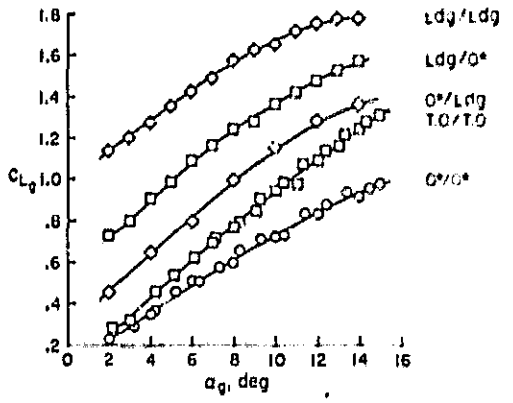


Fig. 5 Measured lift coefficient on the subsonic transport model as a function of angle of attack for various flap settings.

## Rolling-Moment Measurements

The rolling moments imposed on both following models for various configurations of the generator are presented in Figs. 6 and 7 as a function of the lift coefficient on the subsonic transport model. For the conventional flap configurations, the rolling moment on the following model increases nearly linearly with $C_{L_g}$ up to the beginning of stall on the generator. This result is expected because the shape of the span load distribution is nearly independent of lift over the range of $C_{L_g}$ tested, and only the magnitude changes with angle of attack. Since the vortex structure depends directly on the span loading,[6] only the total vortex strength changes with $C_{L_g}$, thereby yielding a nearly linear relationship between $C_{L_g}$ and $C_{l_f}$. It is also interesting to observe in Fig. 6 that the various curves for the conventional configurations lie on approximately the same line. This implies that there is no major change in the vortex structure when one conventional flap configuration is changed to another. An unconventional flap deflection that did not yield a reduction in rolling moment also appears in Fig. 6. For these data, the inboard flap was retracted and the outboard flap was left deflected to the landing setting (labeled 0°/Ldg). Below $C_{L_g} = 1.0$ these data also lie on the same line as the conventional configurations. The change in slope of the $C_{l_f}$ curve above $C_{L_g} = 1.0$ is again associated with wing-tip stall

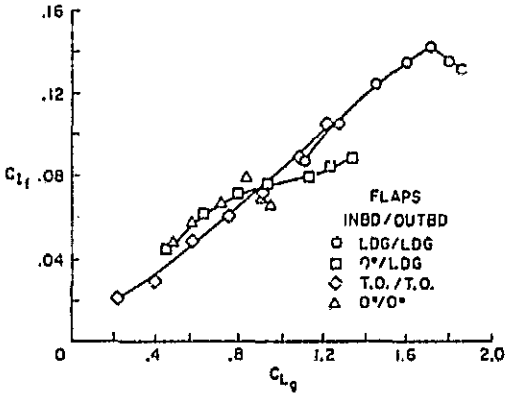


Fig. 6 Variation of peak rolling moment coefficient on following model 1 as a function of lift coefficient on the subsonic transport model for the conventional and outboard-loaded configurations, $b_f/b_g = 0.5$.

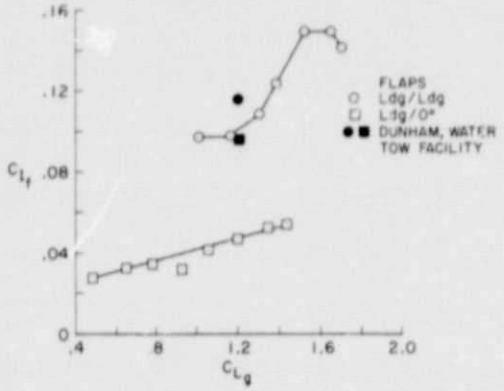


(a) Following model 2, $b_f/b_g = 0.2$.

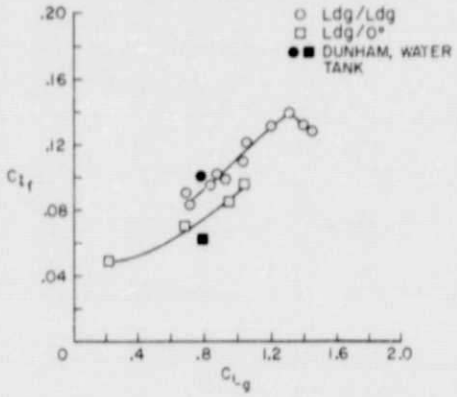


(b) Following model 1, $b_f/b_g = 0.5$.

Fig. 7 Effect of inboard loading on the variation of peak rolling moment coefficient on the following model as a function of lift coefficient on the subsonic transport model.

on the generator. The reason that this outboard loaded configuration was ineffective in reducing $C_{l_f}$ is probably due to the close proximity of the wing-tip vortex of the flap outboard vortex. These vortices can merge with little dispersion, leaving an intense combined vortex.

The Ldg/0°§ configuration, in contrast, produced a substantial reduction in the rolling moment on the smaller following model (Fig. 7(a)) and a modest reduction on the larger following model (Fig. 7(b)). Dunham's data,[13] taken at 14 spans, is seen to be in agreement with the present measurements for the Ldg/Ldg configuration but not for the Ldg/0° configuration. However, at 30 spans downstream and beyond, he shows a reduction in $C_{l_f}$ that is 50% of the Ldg/Ldg configuration. The difference between the two results is believed to be associated with test conditions (near the generator) which lead to variations in the time required for the wake to disperse.

## Flight Test Results

The wind-tunnel results are also in qualitative agreement with recent flight test results[14] conducted by NASA as a consequence of these ground based experiments. The flight experiments were made with a full-scale B747 airplane which could be flown with the flap configurations discussed here. Both a Lear jet and a T37 aircraft were used to probe the vortices of the generator. These aircraft have the same span relative to the B747 as the smaller of the following models in the present paper. The pilots of the probe aircraft reported that, from 4.8 to 8.0 km (3 to 5 mi) behind, the trailing vortices, which were marked by smoke, appeared far more concentrated and well defined for the Ldg/Ldg configuration as compared to Ldg/0°. Furthermore, as a result of flying in the wake at various ranges, they identified a qualitative separation requirement which was much greater for the Ldg/Ldg configuration than for the Ldg/0° configuration. An additional result (which had not been investigated in the ground-based facilities) was obtained in the flight test. It was found that, when either the landing gear of the generator was deployed or the generator was flown with yaw, a substantial part of the benefit of retracting the outboard flap was lost. An explanation for the effect of gear and yaw on the wake structure is now being studied.

## Flow Visualization

Flow visualization studies were conducted in the wind tunnel and in the water tow facility to gain a better understanding of the wake structure. The wake of the conventional flap configuration (Ldg/Ldg) was first studied as a basis for comparison. Figure 8(a) shows a photograph taken at 6 spans downstream. This wake showed a classical arrangement consisting of two concentrated vortex cores connected by a feeding sheet. The accumulation of smoke at the plane of symmetry is caused by the fuselage wake and the vortices from the inboard edge of the inboard flaps. Visualization was conducted over the range from 0 to 13 spans in the wind tunnel and to approximately 40 spans in the water tow facility, however the photograph appearing on Fig. 8(a) is typical of the entire wake aft of about one span. At closer range a vortex pair of opposing sign is visible leaving the region between the inboard and outboard flap on each side of the wing, but this pair has merged into the vortex sheet within one span. Similarly, two vortices of like sign were seen leaving the tip region, one at the flap edge and one closer to the tip. These vortices quickly merge into one within about 1/2 span to form the two intense cores appearing in Fig. 8(a).

Next, the outboard flap was retracted (Ldg/0°). The resulting wake was clearly different from the first configuration studied [Fig. 8(b)]. Three vortices per side were evident. The one that was most intense and well defined originated at the flap outboard edge. The two weaker vortices left the wing tip and flap inboard edge, respectively. The pattern rotated as it moved

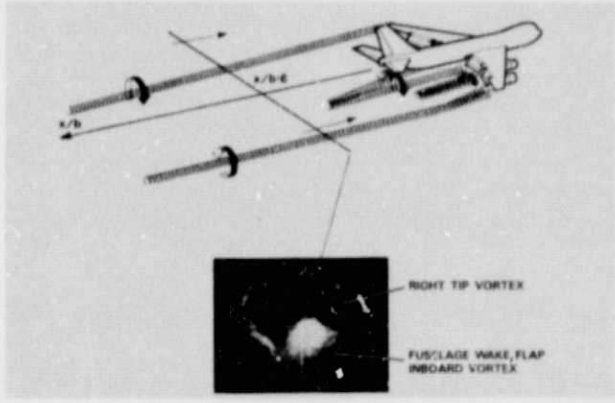


(a) Generator flaps: Ldg/Ldg.

Fig. 8 Light slit photographs of smoke traces in the wind tunnel with an interpretive sketch of the wake at $U_\infty = 12$ m/s (39 ft/s) and $\alpha_g = 4°$.

§This notation means inboard flap set to the landing setting and the outboard flap set to 0°.

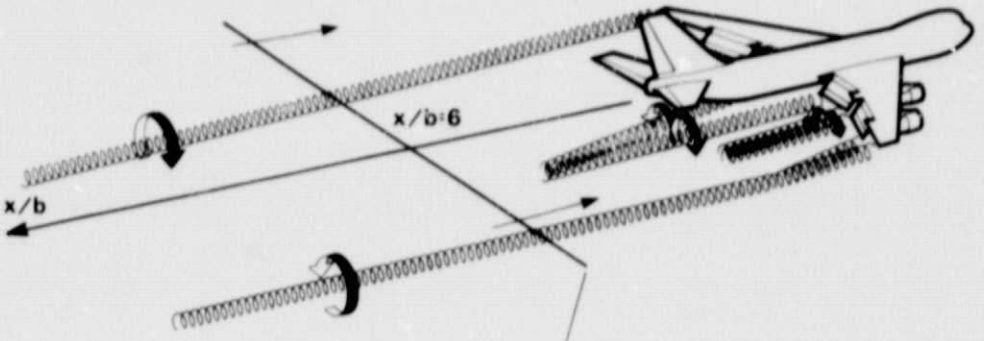


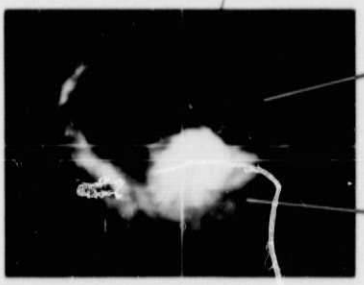


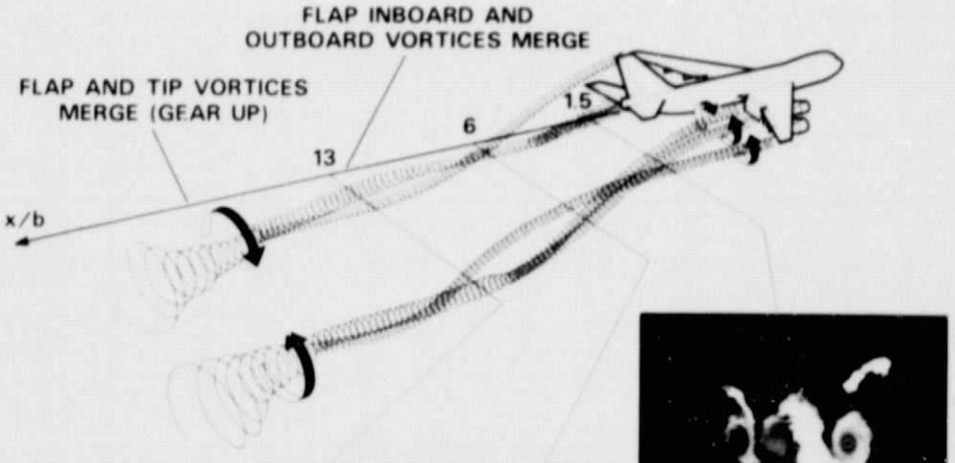




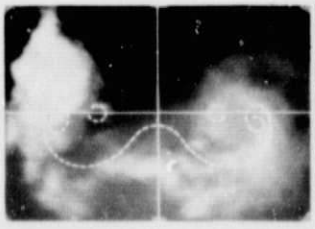

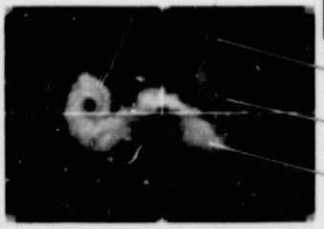

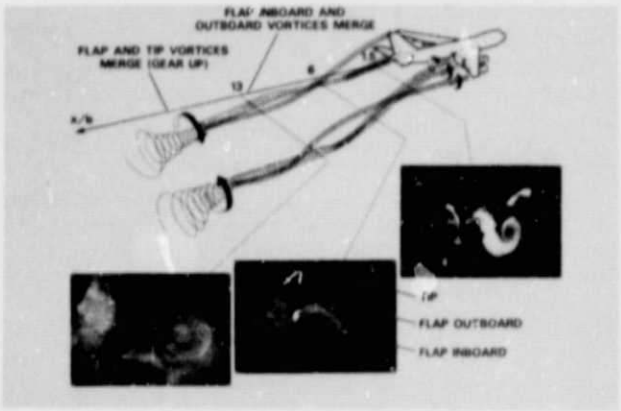


(b) Generator flaps: Ldg/0°.

Fig. 8 Concluded.

downstream, with the tip vortex passing over the flap vortex so that, by 13 spans downstream, it had rotated to a position between the flap vortices. In this same interval, the flap inboard vortices moved under the flap outboard vortices. This inboard vortex was initially diffuse and then diffused further with downstream distance to the extent that, by 13 spans, its presence was barely detectable.

The flap vortex and the tip vortex ultimately merged. This merging was clearly seen in the water tow facility but was beyond the available viewing length in the wind tunnel. Figure 9 shows photographs taken in the water tow facility at the same downstream stations that were used in the wind tunnel as well as at a downstream distance of 32 spans. The agreement of the vortex relative positions between the wind tunnel and the water tow facility at comparable downstream distance is excellent. Beyond $x/b_g = 13$, the wing-tip vortices were seen to continue to rotate an additional 90° around the flap vortices before merging with the flap vortices to become a large, diffuse rotating mass of dye, as can be seen in the photograph at $x/b_g = 32$.

The details of the merging process are not fully understood at the present time. However, as can be seen from the photographs, merging appears to greatly accelerate the dispersion of vorticity. It was generally observed, for example, that a single vortex pair in isolation, as found with the Ldg/Ldg flap configuration, persisted as an organized vortex with a small core until the vortex interacted with the walls of the facility (about 40 span lengths downstream). In contrast, it was found that a wake would disperse rapidly if (i) multiple vortex pairs were shed with initially large spacing, and (ii) the self-induced velocities convected these vortices into close proximity to one another. As shown on Fig. 9, the wing-tip and flap vortices are convected into close proximity between $x/b_g = 1.5$ and $x/b_g = 13$. Next the vorticity of the weak vortex (tip) is convected into an annulus around the strong vortex (flap). This convection is sketched schematically on Fig. 10. Here the vortical region of the weak vortex is taken to be circular at time zero. In the time increments shown, the region is distorted due to the velocity field of the strong vortex. In an example where the two vortices are of comparable strength, the elongation of the core region occurs in both vortices. Furthermore, the elongated core will result in additional distortion due to self-induced velocities. The pairing of vortices of like sign has been studied by Winant and Browand[15] in connection with the instability of a shear layer. They found that in the third stage of mixing layer growth, vortex pairs interacted by rolling around one another to form a single vortex in a manner that is similar to the interactions seen in the present studies.

## Effect of Landing Gear

The effect of the landing gear that was detected in the flight tests was investigated both in the water tow facility and in the wind tunnel. In the wind tunnel, no effect could be detected either in the flow visualization or the rolling moment measurements. In the water tow facility, no effect was detected closer than approximately 30 spans. At greater distances, however, with the landing gear deployed and with the Ldg/0° configuration, the vortex pair was seen to slowly reform into an identifiable core region. With the landing gear retracted, no such reformation occurred. Further research is required to perform measurements of rolling moment or velocity at downstream distances in the range of 25 to 50 spans to adequately explain the landing gear effect. A conjecture is that the axial flow velocity defect in the landing gear wake causes a radial inflow that transports vorticity back to the vortex center.

## Rolling Moment Prediction

Procedure. Prediction of the rolling moment on a following wing is a difficult task, especially when the generating wing is shedding multiple vortices that are undergoing a merging or a partial merging prior to encounter with the follower. A complete theoretical analysis must combine a vortex lattice theory to predict the initial vorticity distribution in the wake with a calculation of the wake rollup and diffusion. The method used to calculate rolling moment in the present paper is a combination of those described by Rossow.[7,16] That is, the structure of the vortex wake and the rolling moment were estimated by completing the following steps:

1. Calculate the span loading on the generating wing from vortex lattice theory.

2. Calculate the vorticity distribution at the wing trailing edge by assuming a flat wake at $x/b_g = 0$.

3. Approximate this vorticity distribution by an array of point vortices and compute the wake rollup to $x/b_g = 3$, using an inviscid, time-dependent, two-dimensional calculation.

4. At $x/b_g = 3$, group point vortices to yield a radial distribution of circulation about each vortex center.

5. Finally, calculate the rolling moment on the following wing using strip theory for each of the vortex groups.

The equations of Ref. 7 are adequate to account for the inviscid merging phenomenon sketched in Fig. 10. Unfortunately, the method is limited by numerical instabilities and by the accumulation of numerical errors so that the calculations were usually terminated at $x/b_g = 3$, which is short of the full downstream distance of interest. These calculations were adequate, however, for estimating the circulation distribution about each of the vortex centers that were identified in the flow visualization. The vortices were then assumed to remain isolated and to proceed without diffusion. The expression for the rolling moment coefficient from strip theory used in step 5 is[16]

$$C_{l_f} = \frac{C_{L_\alpha}}{\pi}\left(\frac{b_c}{b_f}\right)^2 \int_0^{b_f/2b_g} \frac{\Gamma(y)}{b_g U_\infty}\, d(y/b_g) \qquad (1)$$

The $C_{L_\alpha}$ term in Eq. (1) is a variation of the expression given by Jones.[17] Maskew§ reasoned that a wing centered in a vortex

§B. Maskew, Hawker Siddeley Aviation Ltd. (presently NRC Associate at Ames Research Center), private communication.

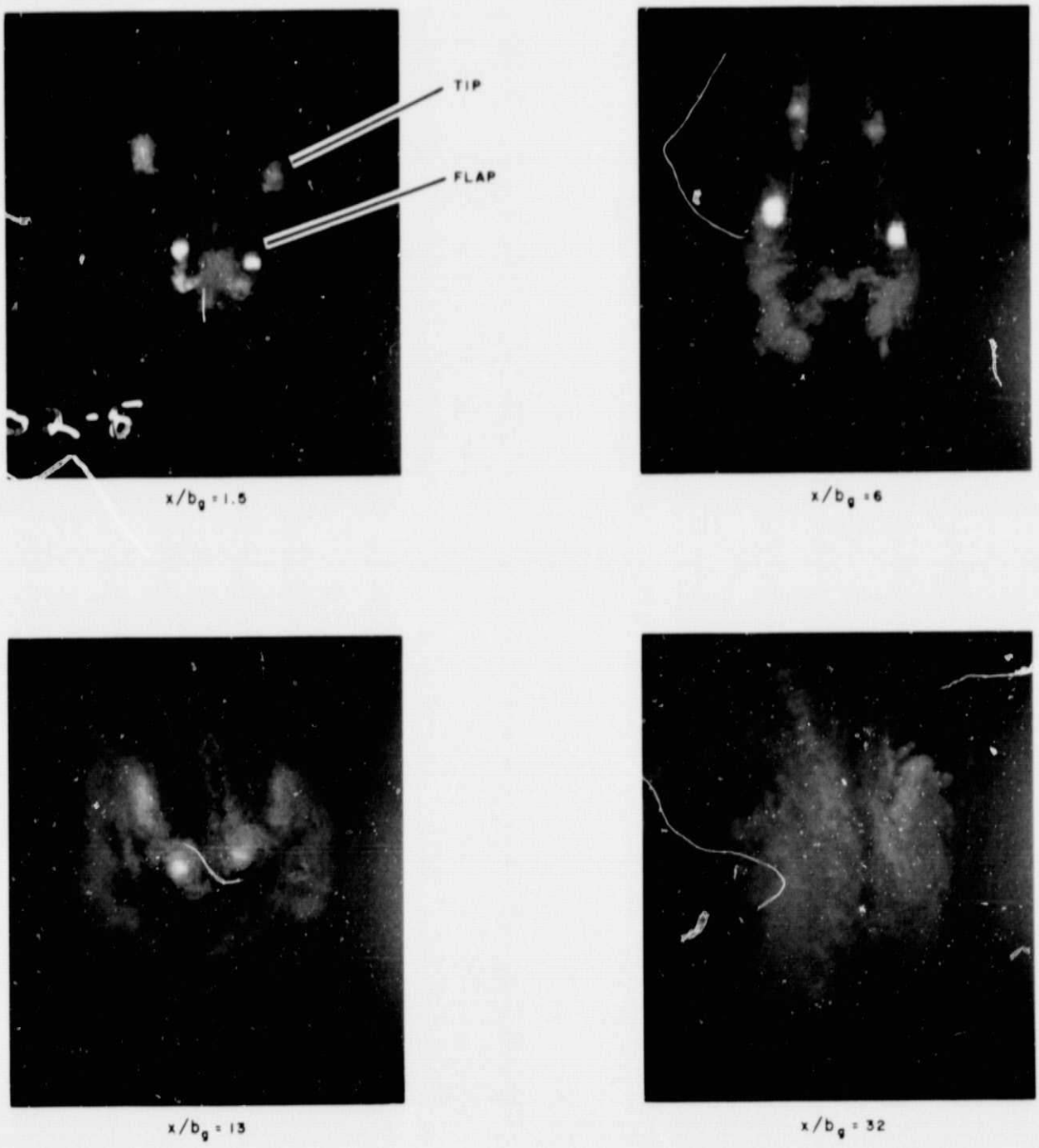


Fig. 9. Light slit photographs of dye traces in the water tow facility, generator flaps: Ldg/0°, $\alpha_g = 5.8°$, $U_\infty = 1$ m/sec (3.3 ft/sec).

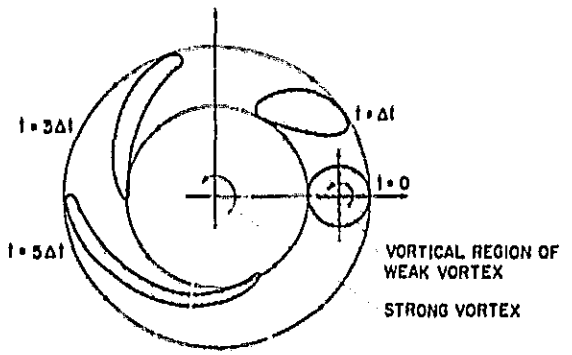


Fig. 10 Idealized convective merging of a weak vortex with a strong one.

would experience an antisymmetric span loading and, therefore, the appropriate interpretation of the Jones expression is to use half the geometric aspect ratio. He confirmed this interpretation by comparison with vortex lattice theory. The resulting expression for $C_{L_\alpha}$ is

$$C_{L_\alpha} = 2\pi AR_f/(AR_f + 6) \qquad (2)$$

Comparison of Results. The foregoing steps and equations were used to calculate the rolling moment on the two following wings for a range of angle of attack of the generating wing when its flaps were deflected to the Ldg/Ldg and the Ldg/0° configurations, respectively. The curves shown in Figs 11(a) and 11(b) for the Ldg/Ldg case are the computed rolling-moment coefficient when the centerline of the following wing coincides with the centroid of vorticity. The theoretical curves are in good agreement with the experimental data. Since this configuration involves one vortex per side, the calculated vorticity distribution approaching the follower involves the least approximation to the real flow, which probably accounts for the good agreement. For the Ldg/0° configuration, two cases were considered [Figs. 11(c) and 11(d)]. Both the wing-tip vortex and the flap outboard-edge vortex were considered in isolation. The experimental data for the larger follower are closest to the theoretical estimate, based on the flap vortex alone, whereas the data for the smaller following model are closest to the estimate, based on a wing-tip vortex

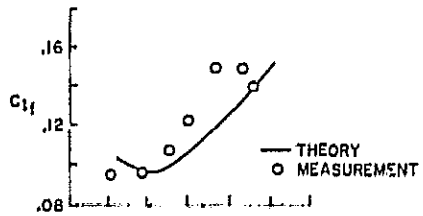


(a) $b_f/b_g = 0.2$, flaps: Ldg/Ldg.

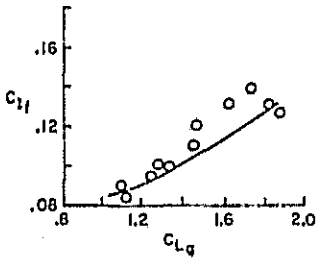


(b) $b_f/b_g = 0.5$, flaps: Ldg/Ldg.

Fig. 11 Predicted rolling moment coefficient compared with present measurements.

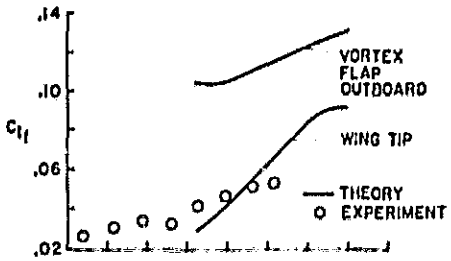


(c) $b_f/b_g = 0.2$, flaps: Ldg/0°.

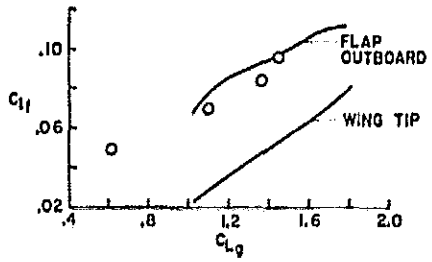


(d) $b_f/b_g = 0.5$, flaps: Ldg/0°.

Fig. 11 Concluded.

penetration. Apparently, as a result of the merging of the flap inboard and flap outboard vortices or as a result of viscous effects, the actual circulation distributions are related to the spans of the followers as sketched on Fig. 12. That is, the flap vortex has greater core size and lower circulation than was obtained using the above theoretical method, which did not account for merging or viscous effects. As shown, the area under the circulation distribution, and therefore $C_{l_f}$, would be larger for the wing-tip vortex if the semispan of the follower were small. With the larger follower, the flap vortex yields the larger $C_{l_f}$. For the curves sketched in Fig. 12, a following wing with semispan equal to $y_c$ experiences the same rolling moment in either vortex.

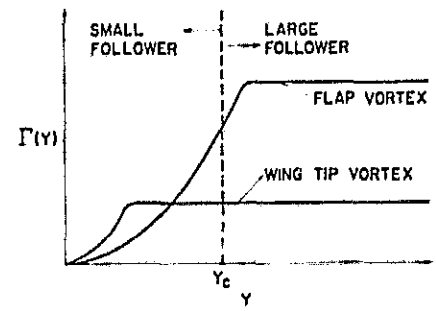


Fig. 12 Sketch of idealized circulation distribution. For $b_f/2 < y_c$, wing tip vortex yields greater $C_{l_f}$. For $b_f/2 > y_c$, flap outboard vortex yields greater $C_{l_f}$.

As noted in the flow visualization, the wing-tip and flap vortices merged at a downstream distance greater than 13.6 spans. Therefore, a prediction of $C_{l_f}$ at the greater downstream distances would have to account for this merger. The predicted $C_{l_f}$ for the fully merged case would be expected to be substantially below that for the conventional configuration at the same lift coefficient of the generator. This can be illustrated by the computation presented in the next subsection.

Merging of Two Vortices. Consider the two idealized span loadings sketched in Fig. 13(a). For the modified configuration,

the wing-tip and flap vortices are assumed to merge into the single circular vortex core with uniformly distributed vorticity (i.e., Rankine vortex). The circulation and core diameter of this merged vortex can be obtained from the vortex invariants attributed to Betz and discussed by Rossow.[6] The rolling-moment coefficient on the follower in the wake of this merged vortex, as well as in the wake of the single vortex of the conventional configuration, can be computed with the aid of Eq. (1) for a given lift coefficient on the generator. This result is shown on Fig. 13(b) as a function of the spacing between the two vortices of the modified configuration. As shown, for vortex spacing in excess of 0.3 of the semispan, the reduction in the rolling-moment coefficient behind the modified configuration, as compared with the conventional configuration, is substantial. The values of $2D/b_g$ of interest are those sufficiently small that merger occurs within a useful downstream distance. If $2D/b_g$ is too large, the flap vortex will move away from the wing-tip vortex under the influence of the flap vortex from the other side of the wing, thereby delaying or eliminating a merger.

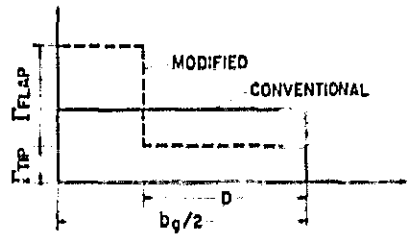


(a) Span loading.

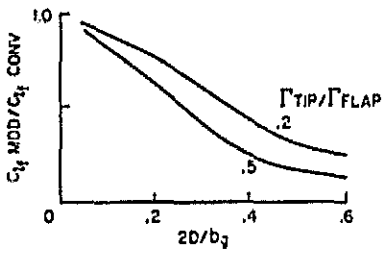


(b) Rolling moment ratio.

Fig. 13 Idealized example of the effect of the merging of two vortices into a single Rankine vortex on the rolling moment coefficient on a follower as compared to a single vortex wake at the same lift and span, $b_f/b_g = 0.2$.

The above examples illustrate that the measured reduction in rolling moment on a follower can be substantially accounted for on the basis of inviscid effects alone. Viscous diffusion of the trailing vortex will further reduce the rolling moment on the follower. The actual relative contribution of viscous and inviscid effects is not known.

## Conclusions

Previous studies of the effect of span loading on wake vortex structure indicated that dispersion of the lift-generated vorticity could be accelerated by modifying the conventional spanwise loadings. The present investigation showed that one of the modifications obtainable with trailing-edge flaps on a model of a subsonic transport was effective in dispersing the wake vorticity so that wings that encounter its wake would experience reduced rolling moments. This configuration was obtained by deflecting only the inboard flaps so that three vortex pairs were shed by the wing. Flow visualization indicated that these vortices ultimately merged into one large, circular vortex by 32 spans downstream of the generator. The merging mechanism discussed here suggests that the reduction in rolling moment is attributable to the merger of multiple vortices that are initially separated from one another by a sizable fraction of the semispan of the generator.

## References


[1] Patterson, J. C., Jr., Lift-Induced Wing-Tip Vortex Attenuation, AIAA Paper 74-38, AIAA 12th Aerospace Sciences Meeting, Washington, D.C., Jan. 1974.

[2] Corsiglia, V. R., Jacobsen, R. A., and Chigier, N. A., An Experimental Investigation of Trailing Vortices Behind a Wing with a Vortex Dissipator, Aircraft Wake Turbulence, Edited by John H. Olsen, Arnold Goldberg, and Milton Rogers. Plenum Publishing Corp., New York, Sept. 1970.

[3] Corsiglia, V. R., Schwind, R. K., and Chigier, N. A., Rapid-Scanning, Three-Dimensional Hot-Wire Anemometer Surveys of Wing-Tip Vortices, Journal of Aircraft, Vol. 10, No. 12, Dec. 1973, pp. 752-757.

[4] Bilanin, A. J., and Widnall, S. E., Aircraft Wake Dissipation by Sinusoidal Instability and Vortex Breakdown, AIAA Paper 73-107, Washington, D.C., 1973.

[5] Chevalier, H., Flight Test Studies of the Formation and Dissipation of Trailing Vortices, Journal of Aircraft, Vol. 10, No. 1, Jan. 1973.

[6] Rossow, V. J., On the Inviscid Rolled-Up Structure of Lift-Generated Vortices, Journal of Aircraft, Vol. 10, No. 11, Nov. 1973, pp. 647-650.

[7] Rossow, V. J., Theoretical Study of Lift-Generated Vortex Wakes Designed to Avoid Rollup, AIAA Journal, Vol. 13, No. 4, April 1975, pp. 476-484.

[8] Ciffone, D. L., and Orloff, K. L., Far-Field Wake-Vortex Characteristics of Wings, Journal of Aircraft, Vol 12, No. 5, May 1975.

[9] Wentz, W. H., Jr., Evaluation of Several Vortex Dissipators by Wind Tunnel Measurements of Vortex-Induced Upset Loads, Wichita State Univ. Aeronautical Rept. 72-3, Sept. 1972.

[10] Singh, B., Kutty, T. M., and Wentz, W. H., Jr., Preliminary Investigation of Rolling Moments Induced by Trailing Vortices for Several Wing-Tip Modifications, Wichita State University Aeronautical Report 72-1, Jan. 1972.

[11] Banta, A. J., Effects of Planform and Mass Injection on Rolling Moments Induced by Trailing Vortices, Master's Thesis, Wichita State Univ., Wichita, Kansas, Dec. 1973.

[12] Iversen, J. D., and Bernstein, S., Trailing Vortex Effects on Following Aircraft, Journal of Aircraft, Vol. 11, No. 1, Jan. 1974, pp. 60-61.

[13] Dunham, E. R., Jr., Model Tests of Various Vortex Dissipation Techniques in a Water Towing Tank, NASA TN (to be published).

[14] Tymczyszyn, J., and Barber, M. R., A Review of Recent Wake Vortex Flight Tests, 18th Annual Symposium of Society of Experimental Test Pilots, Los Angeles, California, Sept. 26, 1974.

[15] Winant, C. D. and Browand, F. K., Vortex Pairing: The Mechanism of Turbulent Mixing Layer Growth at Moderate Reynolds Number, Journal of Fluid Mechanics, Vol. 63, Part 2, 1974, pp. 237-255.

[16] Rossow, V. J., Corsiglia, V. R., Schwind, R. G., Frick, J. K. D., and Lemmer, O. J., Velocity and Rolling-Moment Measurements in the Wake of a Swept Wing Model in the 40- by 80-Foot Wind Tunnel, NASA TM X-62,414, April 1975.

[17] Jones, R. T. and Cohen, D., Aerodynamics of Wings at High Speeds, Aerodynamic Components of Aircraft at High Speeds, Vol. VII, edited by A. F. Donovan and H. R. Lawrence, Princeton University Press, 1957.